Type-III resolver-to-digital converter using synchronous demodulation

Tipo-III conversor resolver-para-digital utilizando a desmodulação síncrona

DOI:10.34117/bjdv8n6-213

Recebimento dos originais: 21/04/2022
Aceitação para publicação: 31/05/2022

Raymundo Cordero García
Doutor em Engenharia Elétrica
Institution: Universidade Federal de Mato Grosso do Sul
Address: Cidade Universitária, s/n, Campo Grande – MS, CEP: 79070-900
E-mail: raymundo.garcia@ufms.br

Edson Antonio Batista
Doutor em Engenharia Elétrica
Institution: Universidade Federal de Mato Grosso do Sul
Address: Cidade Universitária, s/n, Campo Grande – MS, CEP: 79070-900
E-mail: edson.batista@ufms.br

Márcio Afonso Soleira Grassi
Mestre em Engenharia Elétrica
Institution: Universidade Federal de Mato Grosso do Sul
Address: Cidade Universitária, s/n, Campo Grande – MS, CEP: 79070-900
E-mail: marciograssi14@gmail.com

João Onofre Pereira Pinto
Doutor em Engenharia Elétrica
Institution: Oak Ridge National Laboratory
Address: Oak Ridge, Tn 37831, USA
E-mail: pintoj@ornl.gov

ABSTRACT

Resolver is an angular position sensor widely used in applications such as electric/hybrid vehicles, CNCs, antennas and robotics. However, the estimation of the angular position from resolver outputs is more difficult than the analysis of encoder signals, and it is still an open question. Most algorithms proposed in literature are based on type-I or type-II angle tracking ob- servers. Some type-III observers were proposed, but they require a high sampling frequency. This paper explores the use of synchronous demodulation of the resolver outputs to simplify the implementation of a type-III angle tracking observer. The resolver outputs are sampled at the peaks and valleys of the excitation resolver signal, being easy to get sine and cosine of the angular position. The proposed approach reduces the computational cost and the required sampling frequency to implement the type-III observer. Simulation and experimental results prove the accuracy of the proposed approach.

Keywords: angle tracking observer, DSP, resolver, resolver-to-digital converter, type-III observer.

RESUMO
O resolver é um sensor amplamente utilizado em aplicações como veículos elétricos/híbridos, CNC, antenas e robó- tica. Porém, a estimação da posição angular a partir das saídas do sensor é mais complexa que analisar os sinais de um encoder, sendo ainda uma questão aberta. Muitos algoritmos propostos estão baseados em estimadores de ângulo tipo-I e tipo-II. Alguns observadores tipo-III foram propostos, mas precisam de uma alta taxa de amostragem. O presente artigo explora o uso da demodulação síncrona para simplificar a implementação do observador de rastreamento de ângulo tipo-III. As saídas do resolver são amostradas quando o sinal de excitação do resolver atinge seus valores máximos e mínimos, sendo simples obter o seno e cosseno da posição angular. O sistema proposto reduz o custo computacional e a frequência de amostragem necessários para implementar o observador tipo-III. Resultados de simulação e experimentais demonstram a exatidão o observador proposto.

Palavras-chave: observador de rastreamento de ângulo, DSP, resolver, conversor resolver a digital, observador tipo-III.

1 INTRODUCTION

Applications such as CNC (Computer Numeric Control), aircrafts, hybrid/electric vehicles, and robotics work under harsh conditions: high temperature, shocks and vibrations (Lee et. al., 1992; Zhang et. al., 2015; Staebler and Verma, 2017). In these kinds of applications, even with the development of sensorless algorithms, angular position sensors are still used to guarantee the robustness and reliability of the drives, while sensorless techniques can be used as backup systems in case of sensor failure (Cordero et. al., 2017; Filho et. al., 2021).

Resolver is widely used as absolute angular posi- tion sensor for harsh environments as it has long operational lifetime and more robustness than encoders (Kaewjinda and Konghirun, 2006; Wang et. al., 2021). Resolvers can resist shocks up to 200G, vibrations up to 40G and temperatures up to 220°C, while most encoders only resist shocks up to 100G, vibrations up to 10G, and temperatures below 120°C (Jin et. al, 2015).

The resolver outputs are amplitude-modulated signals which give information about the sine and cosine of the angular position. Hence, the decoding of the resolver signals is more difficult than the position sensing using encoders (Sun et. al., 2022). Observers called resolver-to-digital converters (RDCs) are used to get the angular position and speed from resolver signals (Staebler and Verma, 2017). Nowadays, most drives use software-based RDCs which are implemented in the same digital processor

where the control system is implemented, instead of using an additional external hardware (Carusso et. al., 2016; Sabatini et. al., 2019). As resolver outputs are analog signals, the resolution of the angle measurement using resolver depends on the RDC system. Usually, RDCs has a resolution from 10 to 16 bits (Szymczak et. al., 2014).

Most software-based RDCs are based on type-I or type-II closed-loop observers (Idkhajine et. al., 2012; Bergas-Jané et. al., 2012; Qamar et. al., 2015; Wang et. al., 2015; Carusso et. al., 2016). Some of them use oversampling of the resolver signals. In (Bergas-Jané et. al., 2012), it is used a sampling frequency of 288 kHz. On the other hand, some RDCs are based in undersampling demodulation (Idkhajine, et. al., 2009): the resolver outputs are sampled at the peaks and/or valleys of the resolver excitation signal. This method requires low sampling ratio. In (Cordero et. al., 2017), it is proposed a type-III angle tracking observer (ATO) which can track the angular position even for constant acceleration. However, that approach also uses oversampling technique: it is used a sampling frequency of 50 kHz, and the excitation resolver signal multiplies the resolver output signals.

This paper explores the use of synchronous de- modulation of the resolver outputs to reduce the computational complexity of a type-III ATO. The resolver outputs are demodulated by sampling them at the peaks and valleys of the excitation resolver signal. These demodulated signals are used by the ATO to estimate the angular position. The proposed approach reduces the sampling ratio and the computational cost of the RDC, which is a main objective when an algorithm is implemented in a DSP or FPGA. Simulation and experimental results prove the accuracy of the proposed observer.

In this paper, it is not considered the effect of phase or amplitude mismatch in the resolver signals. These problems are the main source of uncertainties in the angle estimation. For example, considering a RDC with a resolution of 12 bits, an amplitude mis- match of 0.3% in the resolver output signals produce an error of 1 LSB (Szymczak et. al., 2014). However, it is possible to apply compensation algorithms to attenuate those problems in the resolver signals (Bergas- Jané et. al., 2012; Noori and Khaburi, 2016). This paper was originally published in the XXII Brazilian Conference on Automation (CBA 2018), as indicated in (Cordero et. al., 2018).

2 ANGLE MEASUREMENT USING RESOLVER

2.1 RESOLVER

Resolver can be modeled as a two-phase machine with an excitation winding (coupled to the motor shaft) and two output windings, according to Fig. 1. The excitation winding receives a high-frequency sinusoidal excitation voltage $v_e(t)$ (Idkhajine et. al., 2012):

$$v_e(\mathrm{t}) = a_e \cos(2\pi f_e t), \qquad (1)$$

where a_e is the excitation amplitude, f_e is the excita- tion frequency (1 to 10 kHz) and t denotes time. The excitation voltage and the movement of the excitation winding produce two amplitude-modulated signals, $v_s(t)$ and $v_c(t)$, in the output windings:

$$v_s(t) = k_e a_e \cos(2\pi f_e t)\sin(\theta), \quad (2) \qquad v_c(t) = k_e a_e \cos(2\pi f_e t)\cos(\theta). \quad (3)$$

Equations (2) and (3) indicate that the resolver out- puts are amplitude modulated signals. Phase or am- plitude mismatch in the resolver signals create uncer- tainties in the angle estimation. For example, consid- ering a RDC with a resolution of 12 bits, an ampli- tude mismatch of 0.3% in the resolver output signals produces an error of 1 LSB (Szymczak et. al., 2014).

2.2 SYNCHRONOUS DEMODULATION

Synchronous demodulation is a undersampling technique to estimate the sine and cosine of the angular position from resolver outputs, as shown in Fig. 2. Data acquisition system is synchronized with the resolver excitation signal $v_e(t)$ so that resolver outputs are sampled at the peaks and/or valleys of $v_e(t)$, i.e., when $v_e(t) = \pm a_e$. Thus, according to (1), (2) and (3):

$$v_s(t) = \begin{cases} k_e a_e \sin(\theta), \text{when } v_s(t) = a_e; \\ -k_e a_e \sin(\theta), \text{when } v_s(t) = -a_e. \end{cases} \qquad (4)$$

$$v_c(t) = \begin{cases} k_e a_e \cos(\theta), \text{when } v_c(t) = a_e; \\ -k_e a_e \cos(\theta), \text{when } v_c(t) = -a_e. \end{cases} \qquad (5)$$

The resolver output samples taken at the excitation signal valleys are multiplied by −1 to compensate the negative value of $v_e(t)$ at those instants. Synchronous

demodulation can be implemented when the excitation signal is generated by the same digital processor used to estimate the angular position.

Figure 1. Scheme of the resolver sensor.

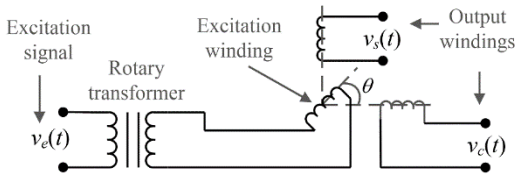

Figure 2. Synchronous sampling of resolver outputs.

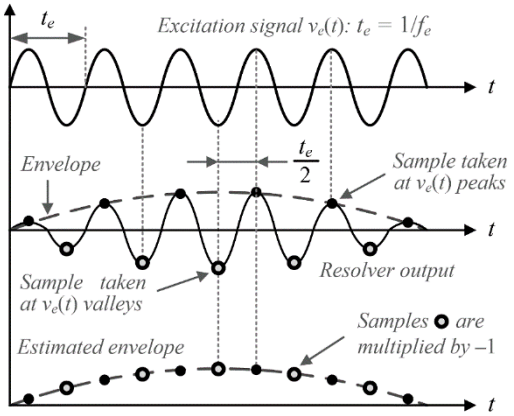

3 PROPOSED APPROACH

Fig. 3 shows the proposed approach. It is composed by the synchronous demodulators and the type-III angle tracking observer (ATO). The integrators are implemented using Backward Euler discretization. In this paper, amplitude or phase mismatches are not considered, as the objective of this paper is to develop an improved ATO. Compensation algorithms (Bergas-Jané et. al., 2012; Noori and Khaburi, 2016) can be used to compensate the mismatch effects.

3.1 DEMODULATION PROCESS

Synchronous demodulation takes samples at both the peaks and the valleys of the resolver excitation, as illustrated in Fig. 4. The square wave represents the sampling instants. It is synchronized with $v_e(t)$, so that their positive and negative transitions happen at the peaks and valleys of $v_e(t)$ respectively. Let $d_s(t)$ and $d_c(t)$ be the envelopes of $v_s(t)$ and $v_c(t)$, respectively. According to (4) and (5) those envelopes are:

$$d_s(t) = k_e a_e \sin(\theta), \qquad (6)$$

$$d_c(t) = k_e a_e \cos(\theta). \qquad (7)$$

When samples of the resolver output are taken at the peaks and valleys of $v_e(t)$, the sampling frequency in synchronous demodulation is twice the resolver excitation frequency, as indicated in (8):

Figure 3. Proposed angle tracking observer.

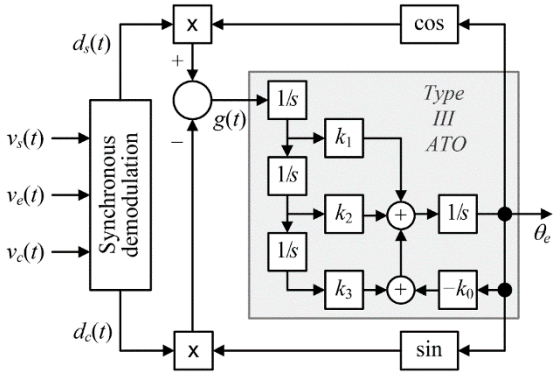

Figure 4. Proposed synchronous demodulation.

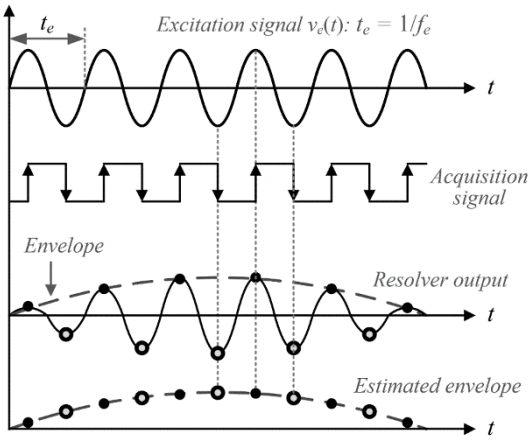

$$f_s = 2f_e. \qquad (8)$$

If only the peaks or valleys were used, the sam- pling frequency would be equal to f_e.

3.2 ANGLE TRACKING OBSERVER

Fig. 3 shows the angle tracking observer (ATO) used in this work, which is based on (Cordero et. al., 2017), but using synchronous demodulation. Assuming that $\theta - \theta_e \approx 0$, $g(t)$ can be approximated as follows:

$$\begin{aligned} g(t) &= k_e a_e \sin(\theta)\cos(\theta_e) - k_e a_e \cos(\theta)\sin(\theta_e) \\ &= k_e a_e[\sin(\theta)\cos(\theta_e) - \cos(\theta)\sin(\theta_e)] \\ &= k_e a_e \sin(\theta - \theta_e) \\ &\approx k_e a_e(\theta - \theta_e). \end{aligned} \quad (9)$$

Equation (10) shows that $g(t)$ is proportional to the estimation error $e_\theta = \theta - \theta_e$. On the other hand, in the oversampling technique (Cordero et. al., 2017), the same signal $g(t)$ is obtained as follows:

$$\begin{aligned} g(t) &= v_e(t)[v_s(t)\cos(\theta_e) - v_c(t)\sin(\theta_e)] \\ &= k_e v_e^2(t)[\sin(\theta)\cos(\theta_e) - \cos(\theta)\sin(\theta_e)] \\ &= k_e v_e^2(t)\sin(\theta - \theta_e) \\ &\approx 0.5 k_e a_e^2\,[1 + \cos(4\pi f_e t)](\theta - \theta_e). \end{aligned} \quad (10)$$

In (10), $g(t)$ is composed by two signals: a low- frequency signal proportional to $e_\theta = \theta - \theta_e$, and a high-frequency signal proportional to $e_\theta \cos(4\pi f_e t)$. It is necessary a low-pass filter (the observer can also act as a filter) to remove the high-frequency signal, for $g(t)$ to be proportional to the angle estimation error, as in (9). For that reason, many samples of the resolver signals must be acquired for the filtering process, and high sampling frequencies are needed.

Based on (9), the ATO in Fig. 3 can be rede- signed as in Fig. 5. Note that the ATO is a type-III system, capable to track even parabolic reference signals. The reference in Fig. 5 is the angular position, while the output is the estimated angle θ_e. Thus, a constant waveform represents a constant position ($\theta = k$), a linear waveform corresponds to a constant speed ($\theta = \omega t$), while a parabolic waveform corresponds to constant acceleration ($\theta = at^2$). From Fig. 5, and based on (Bishop and Dorf, 1998; Cordero et. al., 2017) the closed-loop space-state model of the ATO is described as follows:

$$\dot{\mathbf{E}} = (\mathbf{A} - \mathbf{BK})\mathbf{E} \quad (11)$$

$$\mathbf{A} = \begin{bmatrix} 0 & 0 & 0 & 0 \\ -1 & 0 & 0 & 0 \\ 0 & 1 & 0 & 0 \\ 0 & 0 & 1 & 0 \end{bmatrix}, \quad \mathbf{B} = \begin{bmatrix} k_e a_e \\ 0 \\ 0 \\ 0 \end{bmatrix},$$

$$\mathbf{K} = [k_0 \quad -k_1 \quad -k_2 \quad -k_3], \quad (12)$$

where **E** is the error vector. Control techniques such as Ackermann formula or linear matrix inequalities (LMI) allows setting the poles of (11) and adjust the ATO dynamics. The integrators in Fig. 3 are implemented using Backward Euler discretization:

$$\frac{1}{s} \approx \frac{z}{z-1} t_s, \quad t_s = \frac{1}{f_s} \quad (13)$$

where s is the Laplacian variable, z is the Z-transform variable, and f_s is the sampling frequency.

4 RESULTS

4.1 SIMULATION RESULTS

The proposed angle tracking observer with synchronous demodulation was simulated in MATLAB/SIMULINK. The parameters of the re- solver sensor and the gains are listed in Table 1. The poles of the ATO were set in −40+j40, −40+j40, −35 and −35. The gains of the ATO were set through Ackermann formula. The sampling frequency used in synchronous demodulation and in the discrete integrators is 10 kHz, which is 5 times less than the sampling frequency in (Cordero et. al., 2017). In (Bergas-Jané et. al., 2012), the sampling frequency is 288 kHz. The mechanical speed used in the simulation is shown in Fig. 6: a constant acceleration from 0 to 100 rad/s in 1s, and a constant speed of 100 rad/s.

Figure 5. Simplified structure of the proposed ATO.

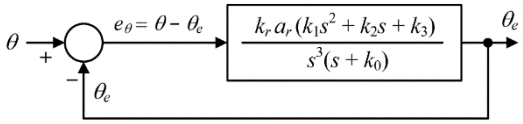

Figure 6. Speed reference.

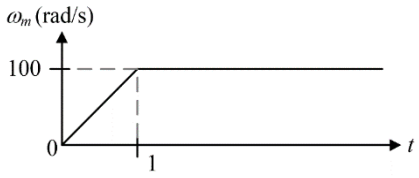

Fig. 7 shows the synchronous demodulation for $v_s(t)$. The demodulated signal is a good estimative of the envelope of the resolver output. The angle estima- tion error is shown in Fig. 8. The steady-state error tends to zero, even for constant acceleration. This result is due to the ATO is a type-III system.

In the second simulation test, white noise (zero mean, variance 2×10^{-4}) was added to the resolver outputs. Figs. 9 and 10 show the simulation results. The steady-state error of the angle estimation is less than 4.40×10^{-3} rad, which is the typical error in industrial applications (Ellis, 2004).

Table 1. Parameters of the Resolver and the ATO.

Parameter	Value
a_e	1 (normalized, p.u.)
k_e	1 (normalized, p.u.)
f_e	5 kHz
f_s	10 kHz (t_s = 0.1 ms)
k_0	150
k_1	10025
k_2	322000
k_3	3920000

Figure 7. Simulation result for synchronous demodulation without noise.

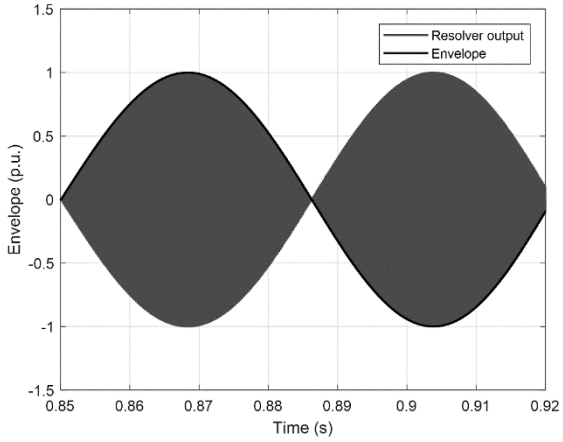

Figure 8. Simulation result for angle estimation error without noise.

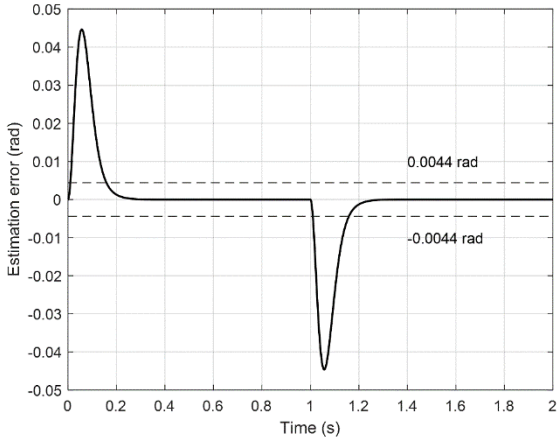

Figure 9. Simulation result for synchronous demodulation with noise.

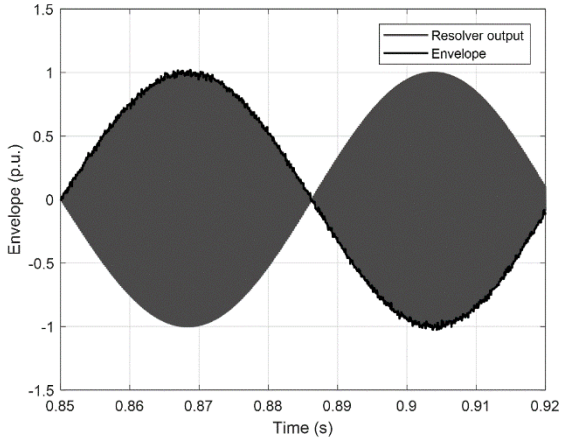

Figure 10. Simulation result for angle estimation error with noise.

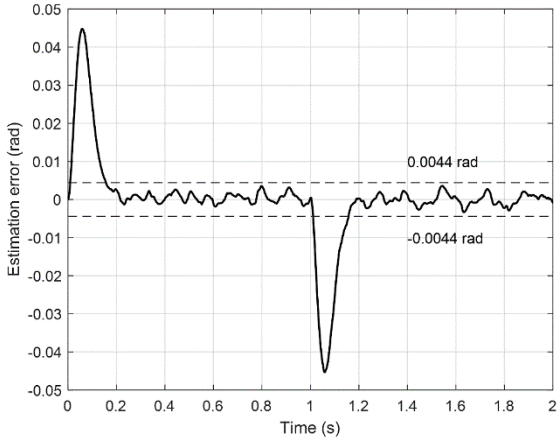

4.2 EXPERIMENTAL RESULTS

The proposed RDC algorithm was experimental- ly implemented in the DSP DSPACE DS1104. The experimental setup is shown in Fig. 11. Following the strategy applied in (Sarma et.al., 2008), the DSP was also used to generate the resolver signals. This strategy allows defining the angular position used in the test, to make an adequate

comparison between the real and the estimated angle (as the angular position is known). Besides, it is possible to test the robustness of the proposed RDC algorithm by adding noise to the resolver signals. The resolver signals were generated using a sampling frequency of 50 kHz.

Figure 11. Experimental setup.

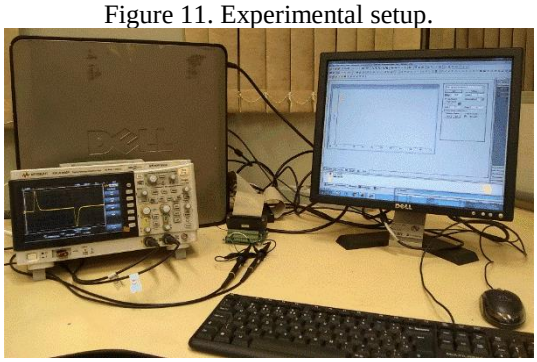

The sampling frequency used in the synchronous demodulation and for the discrete integrators in the ATO was set in 10 kHz, which is 5 times less than the switching frequency used in (Cordero et. al., 2017). The digital-to-analog converters (DACs) of the DSP were used to show the experimental results.

Figs. 12 and 13 show the experimental results for the demodulation process and the angle estimation error without noise. Synchronous demodulation allows getting the envelope of the resolver outputs. As the angle estimation error is small, it was necessary to amplify this error signal before sending it to the DSP DACs. Thus, the vertical scale for error (Fig. 13 and 15) was 160V/rad. An output amplification of 6.4 was also applied to the resolver outputs to improve their visualization. The maximum angle estimation error is $7.175/160 = 4.48\times10^{-2}$ rad, which is similar than the maximum error peak in Fig. 10. The steady-state error tends to zero even during acceleration.

Figs. 14 and 15 show the experimental results of the synchronous demodulation and the angle estimation error when noise (zero mean, variance 2×10^{-4}) is added to the resolver outputs. The peak error in steady-state condition is $0.625/160 = 3.92\times10^{-3}$ rad, which is less than 4.40×10^{-3} rad. Hence, the proposed algorithm can be used to get the angular position from resolver outputs.

Figure 12. Experimental result for synchronous demodulation without noise (vertical scale: 6.4 V/V).

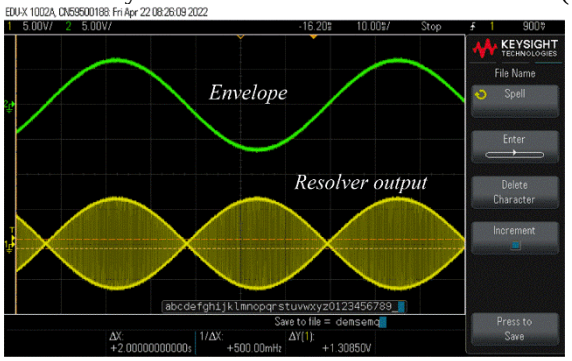

Figure 13. Experimental results for the test without noise (vertical scale: 160 V/rad).

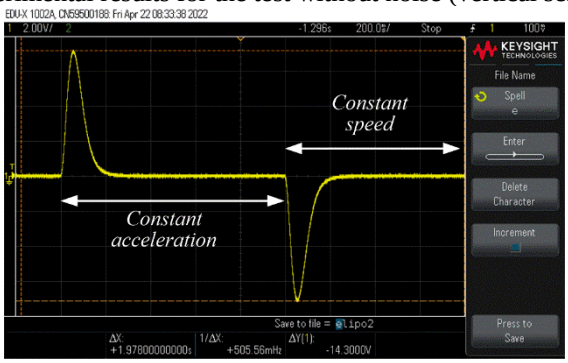

Figure 14. Experimental result for synchronous demodulation with noise (vertical scale: 6.4 V/V).

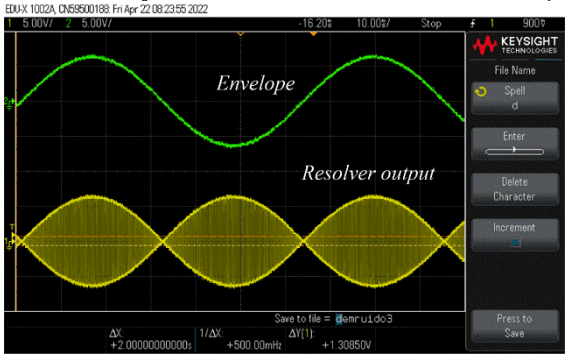

Figure 15. Experimental results for the test with noise (vertical scale: 160 V/rad).

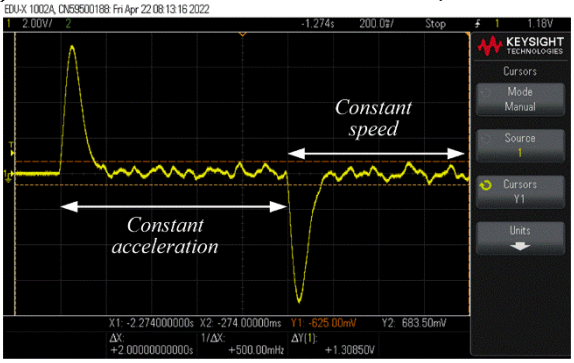

5 CONCLUSION

This paper proposes the use of synchronous demodu- lation of the resolver output signals with the tracking capabilities of a type-III angle tracking observer. The synchronous demodulation allows working with low sampling frequencies, without losing accuracy, which reduces the computational cost of the algorithm. The steady-state angle estimation error is small, even when noise is added. Thus, the proposed algorithm has accuracy, robustness against noise and easy to implement using a low sampling frequency.

ACKNOWLEDGMENT

Authors want to thank BATLAB laboratory - Federal University of Mato Grosso do Sul (UFMS) for the support to this research. This study was financed in part by the Coordenação de Aperfeiçoamento de Pessoal de Nível Superior - Brasil (CAPES) - Finance Code 001.

REFERENCES

Bergas-Jané, J., Ferrater-Simón, C., Gross, G., Ramírez-Pisco, R., Galceran-Arellano, S. and Rull-Duran, J. (2012). High-Accuracy All- Digital Resolver-to-Digital Conversion. IEEE Transactions on Industrial Electronics, vol. 59, no. 1, pp. 326 – 333.

Carusso, M. di Tomasso, A. O., F. Genduso, F., Miceli, R. and Galluzzo, G. R. (2016). A DSP- Based Resolver-to-Digital Converter for High Performance Electrical Drive Applications. IEEE Transactions on Industrial Electronics, Vol. 63, No. 7, pp. 4042 – 4051.

Cordero, R., Pinto, J. O. P., Suemitsu, W. I. and Soares, J. O. (2017). Improved Demultiplexing Algorithm for Hardware Simplification of Sensored Vector Control Through Frequency- Domain Multiplexing. IEEE Transactions on Industrial Electronics, Vol. 64, No. 8, pp. 6583 – 6548.

Cordero, R., Pinto, J. O. P, Batista, E. A. and Grassi, M. (2018). Type-III Resolver-To-Digital Converter Using Synchronous Demodulation. XXII Brazilian Conference on Automation (CBA 2018), pp. 1 – 6.

Dorf, R. C. and Bishop, R. H. (1998). Modern Control Systems, 8th ed., Addison Wesley, pp. 415–665.

Ellis, G. (2004), Control System Design Guide, 3rd. ed., Elsevier, pp. 278 – 292.

Filho, C. J. V., Xiao, D., Vieira, R. P. and Emadi, A. (2021). Observers for High Speed Sensorless PMSM Drives: Design Methods, Tuning Challenges and Future Trends. IEEE Access, Vol. 9, pp. 56397 – 56415.

Idkhajine, L., Monmasson, E., Naouar, M. W., Prata, A. and Boullaga, K. (2009). Fully Integrated FPGA-based Controller for Synchronous Motor Drive. IEEE Transactions on Industrial Electronics, Vol. 56, No. 10, pp. 4006–4017.

Jin, C.-S., Jang, I.-S., Bae, J.-N., Lee, J. and Kim, W.-H. (2015). Proposal of Improved Winding Method for VR Resolver. IEEE Transactions on Magnetics, Vol. 51, No. 3, pp. 1–4.

Kaewjinda, W. and Konghirun, M. (2006). A DSP – Based Vector Control of PMSM Servo Drive Using Resolver Sensor. IEEE Region 10 Conference, pp. 1 – 4.

Noori, N. and Khaburi, D. A. (2016). Diagnosis and compensation of amplitude imbalance, imperfect quadrant and offset in resolver signals. 7th Power Electronics and Drive Systems Technologies Conference, pp. 76 – 81.

Qamar, N. A., Hatziadoniu, C. J. and Wang, H. (2015). Speed Error Mitigation for a DSP-Based Resolver-to-Digital Converter Using Autotuning Filters. IEEE Trans. Ind. Electron., Vol. 62, No. 2, pp. 1134 – 1139.

Sarma, S., Agrawal, V. K. and S. Udupa, S. (2008). Software-based Resolver-To-Digital Conversion Using a DSP. IEEE Transactions on Industrial Electronics, Vol. 55, No. 1, pp. 371 – 379.

Staebler, M. and Verma, A., 2017. TMS320F240 DSP Solution for Obtaining Resolver Angular Position and Speed, Texas Instruments Application Report SPRA605A.

Sun, L., Luo, Z., Hang, J., Ding, S. and Wang, W. (2022). A Slotless PM Variable Reluctance Resolver With Axial Magnetic Field. IEEE Transactions on Industrial Electronics. Vol. 69, No. 6, pp. 6329 – 6340.

Szymczak, J., O'Meara, S., Gealon, J. S. and De La Rama, C. N. (2014). Precision Resolver-to- Digital Converter Measures Angular Position and Velocity. ANALOG Devices – ANALOG DIALOGUE, Vol. 48, No. 3, pp. 1 – 6.

Sabatini, V., Di Benedetto, M., and Lidozzi, A. (2019). Synchronous Adaptive Resolver-to Digital Converter for FPGA-Based High-Performance Control Loops. IEEE Transactions on Instrumentation and Measurement. Vol. 68, No. 10, pp. 3972 – 3982.

Wang, Y., Zhu, Z. and Zuo, Z. (2015). A Novel Design Method for Resolver-to-Digital Conversion. IEEE Transactions on Industrial Electronics, Vol. 62, No. 6, pp. 3724 – 3731.

Wang, R., Wu, Z. and Shi, Y. (2021). Suppressing Harmonics in Resolver Signals via FLL-Based Complementary Filters. IEEE Access. Vol. 9, pp. 158402 – 158411.

Zhang, Z., Ni, F., Dong, Y., Guo, C., Jin, M. and Liu, H. (2015). A Novel Absolute Magnetic Rotary Sensor. IEEE Transactions on Industrial Electronics, Vol. 62, No. 7, pp. 4408 – 4419.